Structure and stereochemistry of products of hydroxylation of human steroid hormones by a housefly cytochrome P450 (CYP6A1). Magn Reson Chem

ARTICLE *in* MAGNETIC RESONANCE IN CHEMISTRY · APRIL 2006

Impact Factor: 1.18 · DOI: 10.1002/mrc.1767 · Source: PubMed

5 AUTHORS, INCLUDING:

Katalin E. Kövér
University of Debrecen
191 PUBLICATIONS **2,216** CITATIONS
SEE PROFILE

F(rances) Ann Walker
The University of Arizona
242 PUBLICATIONS **8,711** CITATIONS
SEE PROFILE

MAGNETIC RESONANCE IN CHEMISTRY
Magn. Reson. Chem. 2006; **44**: 467–474
Published online 12 January 2006 in Wiley InterScience (www.interscience.wiley.com). DOI: 10.1002/mrc.1767

MRC

Structure and stereochemistry of products of hydroxylation of human steroid hormones by a housefly cytochrome P450 (CYP6A1)

Neil E. Jacobsen,[1]* Katalin E. Kövér,[2] Marat B. Murataliev,[1] René Feyereisen[3†] and F. Ann Walker[1]

[1] Department of Chemistry, University of Arizona, Tucson, AZ 85721, USA
[2] Department of Inorganic and Analytical Chemistry, University of Debrecen, Debrecen, Hungary, Europe
[3] Department of Entomology, University of Arizona, Tucson, AZ 85721, USA

Received 4 November 2005; Accepted 7 November 2005

The structure and stereochemistry of nine steroid metabolites isolated in quantities ranging from 0.15 to 1.8 mg were determined using a variety of NMR techniques, including heteronuclear multiple bond correlation (HMBC) using broadband adiabatic ^{13}C pulses and phase-sensitive data presentation. Testosterone, androstenedione and progesterone were oxidized with housefly cytochrome P450 6A1 enzyme reconstituted *in vitro* with housefly NADPH cytochrome P450 reductase and cytochrome b_5. NMR analysis in CD_3OD using a modified HMBC sequence as well as 2D heteronuclear single quantum correlation (HSQC), COSY and nuclear Overhauser and exchange spectroscopy (NOESY), combined with a detailed analysis of J couplings showed that hydroxylation occurs exclusively on the β-face of the steroids, at positions 2, 12, and 15. Copyright © 2006 John Wiley & Sons, Ltd.

KEYWORDS: NMR; ^1H; ^{13}C; insect cytochrome P450; steroids; hydroxylation; steroid A-ring conformation; HMBC; broadband adiabatic shaped pulses

INTRODUCTION

Cytochromes P450 belong to a superfamily of heme protein monooxygenases with heme iron ligated to the thiolate of cysteine.[1] P450 enzymes are vitally important in human health and have potential use in biotechnology as a source of metabolites required for toxicological and pharmacological studies, or as a tool in bioremediation or biocatalysis. Such potential application in turn requires detailed characterization of the substrate specificity and efficient, sensitive techniques for product identification and characterization. In this study we have used CYP6A1, an insect cytochrome P450 with very wide substrate specificity,[2,3] as a model enzyme to characterize oxidation of a different class of substrates, the human steroid hormones testosterone, progesterone and androstenedione. Identification of the products of these hydroxylation reactions by NMR spectroscopy is the purpose of the present paper.

A large number of hydroxylated steroid hormones has been analyzed by NMR spectroscopy[4–10] and X-ray crystallography,[11] including several of the hydroxylation products analyzed in this study. Because much of these data were incomplete and were published before high fields and modern methods of assignment were available, we undertook the complete NMR analysis and assignment, including stereochemistry, of all nine purified products. Elucidation of the structure and stereochemistry of the hydroxylated products was accomplished using 2D heteronuclear single quantum correlation (HSQC),[12] a modified heteronuclear multiple bond correlation (HMBC)[13] experiment, double-quantum filtered correlation spectroscopy (DQF-COSY)[14] and nuclear Overhauser and exchange spectroscopy (NOESY)[15] as well as detailed analysis of ^1H vicinal coupling constants and dihedral angles obtained from energy minimized model structures.

Because of the small quantities of metabolites involved, we had difficulty observing weak HMBC correlations and explored modified pulse sequences to provide greater contrast between weak crosspeaks and noise. The original HMBC experiment[13] uses magnitude-mode presentation in F_2, which gives broader peaks and affords no contrasts between weak crosspeaks and noise since all data are positive. The first gradient-enhanced version of HMBC[16] also uses magnitude mode presentation. There are many other ways in which gradients can be implemented into HMBC/HMQC experiments;[17,18] however, except in the HMQC sequence,[17] the evolution of ^1H chemical shifts during the single long delay for long-range J_{CH} evolution leads to large first-order

*Correspondence to: Neil E. Jacobsen, Department of Chemistry, P.O. Box 210041, University of Arizona, Tucson, AZ 85721-0041, USA. E-mail: neil@email.arizona.edu
†INRA Centre de Recherches d'Antibes, France.
Contract/grant sponsor: National Institutes of Health; Contract/grant numbers: GM39014, ES06694.
Contract/grant sponsor: NSF U.S.-Hungary Collaborative Research; Contract/grant number: INT-0122172.

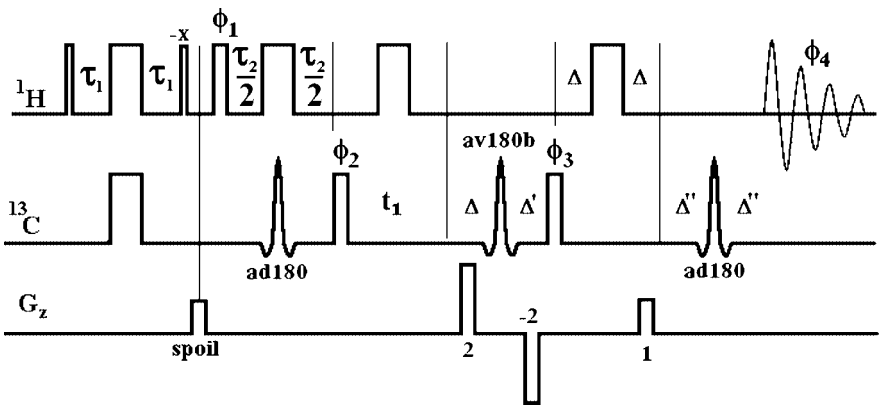

Figure 1. Pulse sequence diagram for the modified HMBC experiment used in this work. Wide pulses are 180°, medium pulses are 90° and narrow pulses are 45°. All pulse phases are *x* unless otherwise indicated. Delays: $\tau_1 = 3.7$ ms; $\tau_2 = 50$ ms; Δ = gradient duration (1.0 ms) + gradient recovery delay (0.5 ms); $\Delta' = \Delta + \tau(180_H)$; $\Delta'' = \Delta + \tau(90_H) + \tau(\text{av180b})/2 - \tau(\text{ad180})/2$. Phases: Φ_1 = x, x, x, x, −x, −x, −x, −x; Φ_2 = x, −x; Φ_3 = x, x, −x, −x; Φ_4 = x, −x, −x, x, −x, x, x, −x. The experiment was performed twice for each t_1 value: first as shown and second with Φ_2 and Φ_4 phases, and the polarity of the first two gradients inverted. Each pair of FIDs was then combined to generate pure cosine and sine modulation in t_1.

phase errors in the F_2 dimension. We modified a gradient-selected HMBC pulse sequence[16] for phase-sensitive data presentation with all undesired chemical shift evolution refocused. In principle, pure absorption-mode phase can be obtained with this sequence using a 90° ^{1}H purging pulse[19] to eliminate antiphase terms with respect to homonuclear couplings, but as this can lead to significant loss of sensitivity we omitted this feature. Our modified HMBC pulse sequence incorporates ad180 ('cawurst') adiabatic shaped pulses[20] for ^{13}C inversion and av180b ('Ivega') shaped pulses[20] for ^{13}C refocusing in order to achieve uniform ^{13}C excitation at 14.1 T (Fig. 1).

EXPERIMENTAL

Recombinant housefly CYP6A1, P450 reductase and cytochrome b_5 were expressed in *Escherichia coli* and purified as previously described.[21,22] Reconstitution of the purified proteins was carried out as detailed earlier.[21]

Enzymatic activity of CYP6A1 was measured in 100 µl of reaction mixture containing 100 µM testosterone, 50 µM NADPH, NADPH-regenerating system, and 0.02 µCi of [^{14}C] testosterone. After addition of the reconstituted enzyme mixture and incubation for 5 min at 25 °C, 100 µl of MeOH containing 10% of 5 N HCl was added and 100 µl of this mixture was applied to a Supelco C18 HPLC column at 1 ml/min flow rate. A gradient was developed as follows: 0–5 min 50% A, 50% B, 5–25 min a linear gradient of 50–100% B followed by 5 min 100% B, where solvent A is water and solvent B is acetonitrile/water/acetic acid; 50/50/0.05. Chromatography was monitored both by absorption at 240 nm and by flow-through radioactivity detection (Fig. 2). Similar procedures were used for oxidation of androstenedione and progesterone.

To obtain quantities of metabolites suitable for NMR analysis, products of steroid oxidation were purified from 0.5–1.0 l of the reaction mixtures incubated overnight. The unreacted substrates and oxidation products were isolated by solid phase extraction using 500 mg C18 reverse phase

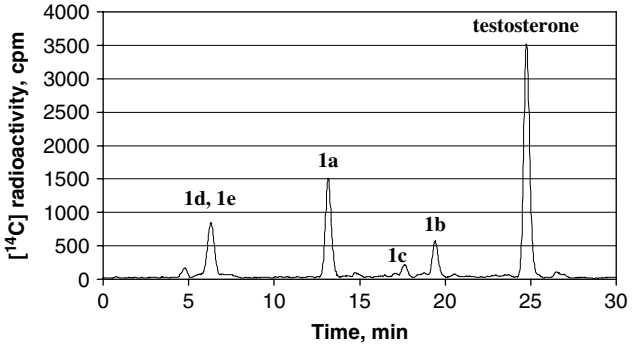

Figure 2. HPLC elution profile of products of testosterone hydroxylation by CYP6A1. The reaction was carried out in the presence of 0.075 µM CYP6A1, 0.67 µM P450 reductase, 1.0 µM of holo-b_5, 100 µM testosterone, 50 µM NADPH, and NADPH regenerating system. No reaction products were detected if either CYP6A1 or P450 reductase was omitted, and the presence of NADPH was absolutely required for the reaction to occur.

columns (Burdick and Jackson). After sample (20–25 ml) application, the columns were washed with 5 ml water, and metabolites were eluted with 8 ml of MeOH. The eluates were pooled, dried under vacuum, dissolved in 50% MeOH, and metabolites were purified by reversed phase HPLC. For monohydroxylated products the analytical gradient described above was used. The same solvents were used for separation of dihydroxytestosterones using the following gradient at 1 ml/min: 0–4 min, 90% A, 10% B; 4–110 min, a linear gradient of 10 to 45% B, 110–120 min, a linear gradient of 45 to 100% B; followed by 5 min 100% B. Retention times were 72.5 min for **1e**, 78.8 min for **1d**, and 76.1 min for a minor unidentified dihydroxytestosterone. Fractions from several HPLC runs were pooled and dried under vacuum. Similar protocols were used for isolation and purification of the products of oxidation of progesterone and androstenedione.

Samples were dissolved in 0.6 ml of CD_3OD for NMR analysis. A sample of **1b** was also prepared in $CDCl_3$

for comparison with literature data.[5,6] Most ^{1}H-detected NMR spectra were acquired on a Bruker Avance DRX-600 spectrometer operating at a ^{1}H frequency of 600.13 MHz, using a 5-mm Bruker TXI triple-resonance 3-axis gradient probe. ^{13}C and DEPT spectra were acquired on a Bruker Avance DRX-500 spectrometer operating at a ^{1}H frequency of 499.93 MHz, using a 5-mm Bruker dual ^{13}C-detect probe. The modified HMBC experiment was optimized using a Varian Inova-600 spectrometer operating at a ^{1}H frequency of 599.7 MHz, with a 5-mm HCN *Z*-axis gradient probe. Samples were analyzed in 5 mm NMR tubes at 25 °C with spinning for 1D experiments and without spinning for 2D experiments. 1D ^{1}H spectra were acquired with a spectral width of 7507.5 Hz, acquiring 8192 complex data points. Sample quantities were estimated by comparing absolute integrals of resolved single-proton peaks with a calibration curve derived from 10 different concentrations of sucrose in D_2O. 2D spectra were acquired in TPPI mode[23] (gradient-selected edited HSQC[17]), States mode[24] (NOESY and Varian gradient-selected DQF-COSY[25]) or echo-antiecho mode[26] (HMBC and Bruker gradient-selected DQF-COSY[25]) with 1024 complex pairs in t_2 and 750 FIDs. All NMR data were processed using the Felix2000 software (Accelrys Inc., San Diego, CA). ^{1}H chemical shifts are referenced to residual CHD_2OD at 3.30 ppm and ^{13}C chemical shifts are referenced to solvent CD_3OD at 49.15 ppm (1D spectra) or residual CHD_2OD at 49.43 ppm (2D spectra). *J*-coupling analysis of 1D ^{1}H spectra was done using an unshifted sinebell window and zero-filling from 8192 to 32 768 complex data points before Fourier transformation, for a final digital resolution of 0.23 Hz/point. 2D data were zero-filled to a final matrix size of 2048 data points in F_2 and 1024 data points in F_1, using (in both dimensions) a skewed, 45°-shifted sinebell window function for HSQC, a 90°-shifted sinebell for HMBC and NOESY and an unshifted sinebell for DQF-COSY.

The modified HMBC pulse sequence is shown in Fig. 1. This sequence is based on the gradient-selected HMQC sequence[16] designed for phase-sensitive data presentation, with a TANGO[27] element and gradient at the beginning to eliminate ^{13}C-bound ^{1}H coherence. The refocusing period just prior to acquisition is eliminated to minimize signal loss due to ^{1}H T_2 relaxation, and the ^{13}C spin-echo period is shortened to allow just enough time (Δ) for a gradient and its recovery delay in each of the two delay periods. After conversion of multiple quantum coherence (MQC) back to ^{1}H single quantum coherence (SQC) a short (2Δ) ^{1}H spin-echo is added, followed by another ^{13}C spin-echo which refocuses ^{1}H chemical shift evolution which occurred during the first ^{13}C spin-echo. To achieve uniform excitation over the ^{13}C spectral window, all three ^{13}C 180° pulses were converted into broadband shaped pulses.

Shaped pulses were calibrated and optimized using a doped $^{13}CH_3I$ in $CDCl_3$ sample on a Varian Inova-600. The pulse shapes were calculated in the pulse sequence using the Pandora's Box program with a 1.0 μs step size. The ad180 ^{13}C adiabatic inversion pulse[20] was optimized using the sequence: 180° (shaped) – 90° (hard) – FID(^{1}H-dec.). Excellent inversion up to 120 ppm (18 kHz) off-resonance was obtained with a pulse width of 477 μs and a maximum B_1 amplitude of 15.7 kHz. The av180b ^{13}C refocusing pulse[20] was optimized using a ^{13}C DPFGSE[28] (double pulsed field gradient spin-echo), setting the shaped pulse 90 ppm (13.5 kHz) off-resonance and varying the pulse width with the maximum power held constant. The best results were obtained with a pulse width of 273 μs (19.1 times the 90° pulse width of the corresponding hard pulse, instead of the theoretical ratio[20] of 24.8) and a maximum B_1 amplitude of 17.5 kHz.

Structure calculations were performed on a Silicon Graphics Octane workstation using the Insight II software package (Accelrys, Inc., San Diego, CA). Structures were built using the Builder module and minimized using the Optimize command. Energy minimization uses the consistent valence force field (CVFF) with 1000 steps of steepest descent followed by 1000 steps of conjugate gradient and finally 1000 steps using the Broyden-Fletcher-Goldfarb-Shanno (BFGS) algorithm.

RESULTS

Steroid metabolism by CYP6A1 and isolation of metabolites

The [^{14}C] elution profile of the testosterone hydroxylation reaction is shown in Fig. 2. Incubation with reconstituted CYP6A1 resulted in the formation (Scheme 1) of three major products: 15β-hydroxytestosterone (**1a**), 2β-hydroxytestosterone (**1b**), and 12β-hydroxytestosterone (**1c**), as well as two minor dihydroxylated products: 2β,15β-dihydroxytestosterone (**1d**) and 12β,15β-dihydroxytestosterone (**1e**). The dihydroxy products were separated in a subsequent HPLC purification step (data not shown).

Similarly, progesterone and androstenedione were also oxidized by CYP6A1 (Scheme 1). Only two products were detected with androst-4-ene-3,17-dione as a substrate: 15β-hydroxyandrost-4-ene-3,17-dione (**2a**) and 2β-hydroxyandrost-4-ene-3,17-dione (**2b**), while progesterone oxidation resulted in two major products, 15β-hydroxyprogesterone (**3a**) and 2β-hydroxyprogesterone (**3b**), and a minor product which was not isolated. The estimated quantities in the NMR samples were 0.73, 0.19, 0.47, 0.47, 1.8, 0.33, 0.25, 0.26 and 0.15 mg for samples **1a**, **1b**, **1c**, **1d**, **1e**, **2a**, **2b**, **3a**, and **3b**, respectively.

Structure and stereochemistry of metabolites

To determine regio- and stereospecificity of steroid oxidation, the reaction products (0.15–1.8 mg) were analyzed by NMR spectroscopy in CD_3OD solution. Complete assignment of all ^{1}H and ^{13}C signals was accomplished for all 9 hydroxylated steroids using the 2D HSQC, HMBC and COSY data at 600 MHz (Tables 1 and 2). ^{1}H–^{1}H coupling constants, derived from analysis of 1D ^{1}H spectra, are given in Table 3. ^{1}H chemical shifts of **1b** in $CDCl_3$ were identical to literature values.[5,6] Details of ^{1}H multiplicities and 2D HMBC and COSY correlations for each of the nine products are given in the supplementary material, Tables S1–S9. Regiochemistry of hydroxylation could be determined from ^{1}H coupling patterns of the downfield-shifted H–C–(OH) protons and from the HMBC correlations of these protons and their attached carbons. Each of the three hydroxylation positions (2, 12 and 15) give unique multiplet patterns and chemical

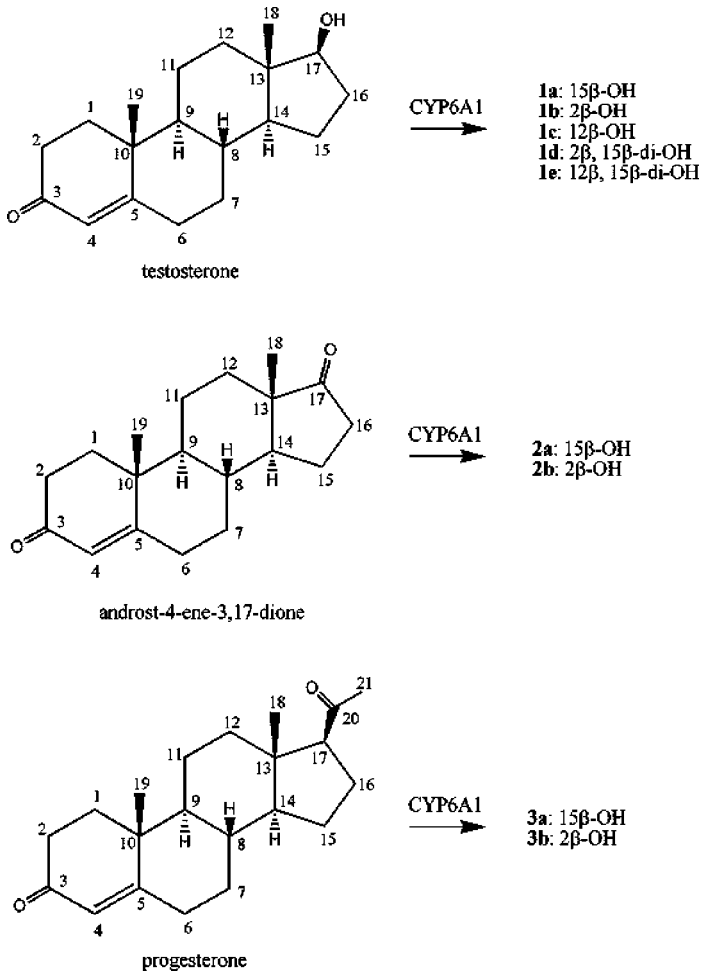

Scheme 1

Table 1. ^{1}H chemical shifts[a]

	1a	1b	1c	1d	1e	2a	2b	3a	3b
1α	1.700	2.312	1.708	2.315	1.718	1.714	2.307	1.721	2.316
1β	2.090	1.622	2.067	1.648	2.074	2.095	1.646	2.097	1.634
2α	2.285	4.174	2.291	4.175	2.298	2.294	4.184	2.295	4.196
2β	2.490	–	2.485	–	2.497	2.496	–	2.493	–
4	5.710	5.713	5.709	5.723	5.720	5.735	5.740	5.720	5.725
6α	2.306	2.250	2.305	2.264	2.320	2.367	2.306	2.320	2.260
6β	2.537	2.570	2.472	2.615	2.521	2.568	2.619	2.531	2.580
7α	1.053	1.009	0.968	1.069	1.031	1.183	1.134	1.118	1.071
7β	2.176	1.982	1.874	2.302	2.176	2.219	2.112	2.191	1.997
8	2.030	1.745	1.609	2.126	1.979	2.142	1.920	1.993	1.735
9	0.995	1.391	1.044	1.427	1.084	1.075	1.470	1.069	1.463
11α	1.596	1.743	1.685	1.729	1.656	1.695	1.827	1.666	1.801
11β	1.480	1.560	1.456	1.577	1.446	1.550	1.586	1.515	1.576
12α	1.043	1.147	3.440	1.113	3.365	1.270	1.337	1.480	1.555
12β	1.828	1.886	–	1.846	–	1.749	1.812	2.049	2.096
14	0.824	1.011	0.951	0.855	0.778	1.351	1.389	1.086	1.267
15α	4.144	1.581	1.625	4.110	4.134	4.497	1.944	4.258	1.691
15β	–	1.314	1.416	–	–	–	1.622	–	1.271
16α	2.490	1.975	2.019	2.474	2.512	2.487	2.078	2.160	2.137
16β	1.596	1.476	1.497	1.591	1.604	2.461	2.448	2.195	1.669
17	3.480	3.583	3.819	3.490	3.708	–	–	2.573	2.646
18	1.020	0.787	0.827	1.027	1.056	1.200	0.932	0.898	0.669
19	1.262	1.190	1.242	1.253	1.265	1.286	1.347	1.255	1.216
20	–	–	–	–	–	–	–	2.124	2.118

[a] In CD_3OD, referenced to residual CHD_2OD at 3.30 ppm.

Table 2. ^{13}C chemical shifts[a]

	1a	1b	1c	1d[c]	1e[c]	2a	2b[c]	3a	3b
1	36.97	41.69	36.92	41.84	36.96	36.83	41.71	36.95	41.69
2	34.87	69.92	34.81	69.96	34.85	34.78	69.89	34.87	69.95
3	202.59	201.76	202.42	[b]	[b]	202.31	[b]	202.45	201.65
4	124.24	120.59	124.50	120.59	124.61	124.41	120.92	124.32	120.72
5	175.61	176.46	174.69	176.55	174.80	174.74	175.70	175.25	176.05
6	34.02	33.98	33.97	33.98	33.94	33.76	33.76	34.00	33.98
7	32.45	35.74	32.41	35.11	31.89	31.70	34.86	32.53	36.07
8	32.83	37.21	36.08	33.24	32.00	32.79	36.65	33.08	37.13
9	55.97	52.28	54.21	52.69	54.17	55.67	52.11	55.58	51.95
10	40.38	42.57	40.05	42.85	40.24	40.29	42.58	40.29	42.47
11	21.83	23.60	30.73	23.54	30.60	21.45	23.17	22.20	23.94
12	39.27	37.83	79.88	39.27	80.34	33.95	32.65	41.26	39.83
13	43.47	44.59	48.56	43.99	48.00	48.04	49.47	44.85	45.64
14	56.56	51.88	50.33	56.48	55.12	56.17	52.15	61.55	57.28
15	69.58	24.37	24.03	69.69	69.48	67.56	22.85	70.81	25.46
16	43.68	30.81	30.94	43.84	43.93	48.07	36.80	36.93	24.02
17	81.97	82.31	82.59	81.92	82.09	222.89	[b]	64.88	64.61
18	14.36	11.85	6.71	14.50	8.60	18.21	14.39	16.38	13.95
19	17.81	23.23	17.75	32.20	17.64	17.64	18.48	17.76	23.17
20	–	–	–	–	–	–	–	211.39	212.28
21	–	–	–	–	–	–	–	31.65	31.68

[a] In CD_3OD, referenced to residual CD_3OD at 49.15 ppm.

[b] Not observed in HMBC spectrum.

[c] Chemical shifts from HMBC spectrum, referenced to residual CHD_2OD at 49.43 ppm.

Table 3. $^1H–^1H$ coupling constants in Hz

	1a	1b	1c	1d	1e	2a	2b	3a	3b
1α–1β	13.5	13.8	13.3	13.7	13.5	13.4	13.8	13.4	13.8
1α–2α	4.6	5.2	4.2	5.1	4.4	4.3	5.2	4.5	5.2
1α–2β	14.8	–	?	–	14.2	14.8	–	14.7	–
1β–2α	3.1	12.7	2.9	12.7	3.0	3.3	12.6	3.0	12.7
1β–2β	5.2	–	5.1	–	5.2	5.2	–	5.2	–
2α–2β	17.1	–	17.0	–	?	17.0	–	17.0	–
2α–4	1.0	∼0	1.0	∼0	?	1.0	∼0	∼1	∼0
6α–6β	14.8	12.4	14.8	12.4	?	14.7	12.7	14.6	∼14
6α–7α	4.0	4.2	4.2	4.0	?	4.1	4.5	4.1	4.4
6α–7β	2.5	2.6	2.3	2.8	2.7	2.5	?	2.4	2.5
6β–7α	14.3	13.2	?	13.5	?	13.9	13.7	14.1	12.6
6β–7β	5.5	5.1	?	5.0	5.9	5.5	5.1	5.5	5.0
6β-4	1.9	1.3	∼1	1.3	∼1	1.9	1.5	1.9	1.5
7α–7β	12.6	?	?	12.7	12.6	12.5	12.3	?	12.4
7α–8	11.2	?	?	∼12	11.3	11.6	12.3	11.2	13.4
7β–8	3.2	?	?	3.8	3.4	3.4	?	3.2	4.3
8–9	10.8	10.5	10.8	10.5	11.1	10.8	10.3	11.2	10.5
8–14	11.3	?	11.0	11.2	11.4	11.2	10.9	11.2	?
9–11α	4.2	4.0	4.1	3.8	4.3	4.3	3.8	?	4.2
9–11β	12.1	12.4	12.8	12.4	12.7	12.4	12.5	?	12.3
11α–11β	13.9	∼13	12.8	13.5	12.9	∼13	?	?	?
11α–12α	?	4.2	4.7	4.1	4.4	4.6	4.6	?	?
11α–12β	2.9	2.9	–	2.9	–	2.8	?	?	?
11β–12α	12.9	12.9	11.2	∼13	11.2	∼13	∼13	?	?
11β–12β	4.2	4.1	–	4.0	–	4.2	?	?	?
12α–12β	12.5	12.7	–	12.6	–	12.9	13.1	?	?

(*continued overleaf*)

Table 3. (*Continued*)

	1a	1b	1c	1d	1e	2a	2b	3a	3b
14–15α	5.7	?	7.3	5.7	5.8	4.4	5.9	5.7	?
14–15β	–	12.2	11.9	–	–	–	12.8	–	?
15α–15β	–	~12	12.0	–	–	–	?	–	?
15α–16α	7.9	?	9.1	7.8	8.0	5.6	9.2	7.2	?
15α–16β	2.6	3.6	3.4	2.5	2.7	1.4	0.9	2.5	?
15β–16α	–	5.8	5.8	–	–	–	9.2	–	?
15β–16β	–	12.0	11.9	–	–	–	8.9	–	?
16α–16β	14.4	13.4	13.3	14.4	14.5	19.4	19.4	14.9	?
16α–17	8.8	8.6	9.1	8.6	8.7	–	–	9.0	9.1
16β–17	8.8	8.3	8.0	8.9	8.7	–	–	9.6	9.1

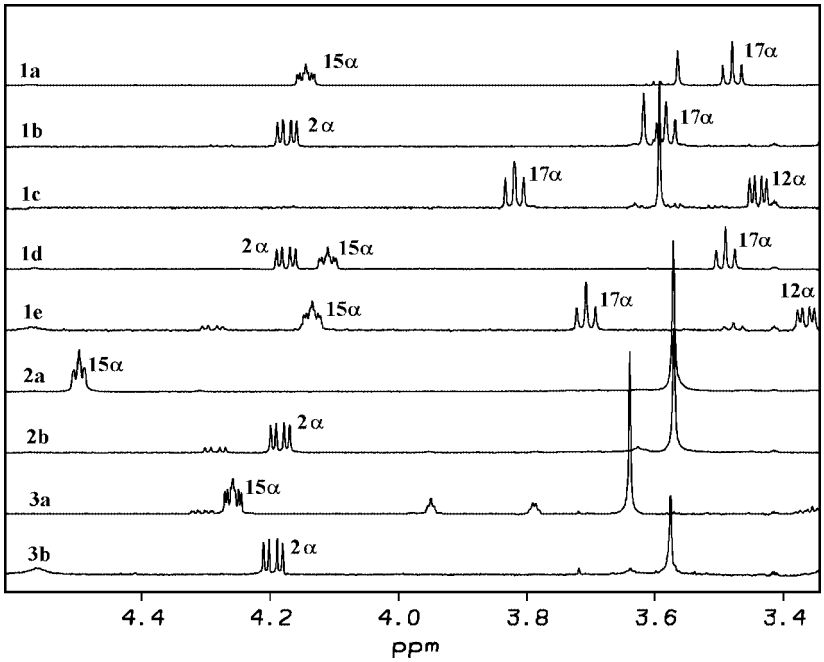

Figure 3. Stacked plot of the HC–(OH) region of the 600 MHz ^{1}H spectra of purified steroid metabolites in CD_3OD at 25 °C, with proton assignments.

shift positions which can be identified from 1D ^{1}H spectra of all 9 metabolites (Fig. 3). NOESY spectra with a 400-ms mixing time were acquired for **1a** and **1b** to confirm the A-ring conformation change. In the 2β-hydroxylated steroid **1b** the H-2α to H-9 crosspeak volume was twice the volume of the H9 to H-12α (1,3-diaxial) crosspeak, while no H-2α to H-9 crosspeak was observed for **1a**. In most cases 1D ^{13}C and DEPT data were also obtained and these confirmed the 2D data, especially in the case of the quaternary carbons. Stereospecific assignments of methylene ^{1}H signals were made by careful *J*-coupling analysis of resolved ^{1}H peaks using resolution enhancement; these were confirmed by the presence or absence of long-range (4-bond) COSY correlations between axial protons and angular methyl groups, and of 3-bond HMBC correlations between axial protons and angular methyl carbons or between equatorial protons and ring carbons.

The modified HMBC sequence presented here gave excellent performance across a wide ^{13}C spectral window at 14.1 T field strength. The phase-sensitive presentation (Fig. 4)

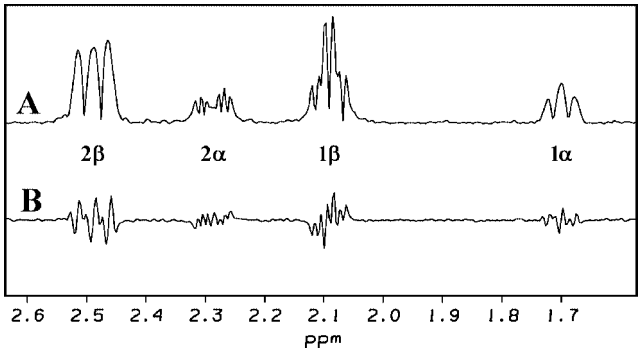

Figure 4. F_2 slices of 2D HMBC spectra of **1a** at the F_1 chemical shift of the C_3 (ketone carbonyl) resonance (95.9 ppm/14.38 kHz off-resonance). (a) Gradient-enhanced HMBC with magnitude mode data presentation, using the sequence of Reference 16. (b) HMBC with phase-sensitive data presentation, using the sequence of Fig. 1. For each experiment 16 scans were acquired for each of 750 FIDs, for a total experiment time of 4.3 h.

affords resolution improvement and contrast with noise for weak signals, with antiphase long-range couplings in F_2 and only mild distortions due to homonuclear couplings.

Structure calculations

Further confirmation of stereospecific assignments was obtained by plotting measured $^3J_{HH}$ couplings against dihedral angles determined from structural models generated by energy minimization (Fig. 5). In the calculated structures there were two distinct energy minima (Fig. 6) corresponding to an A-ring in which C-1 is below the average plane of C2-C5 and C-10 ('C1-α') and to an A-ring with C-2 below the average plane of C-1, C3-C5 and C-10 ('C2-α'). In the C1-α structures, H-1α is roughly *anti* to methyl-19, and H-2β (or HO-2β) is roughly 1,3 diaxial to methyl-19. The H-2α to H-9 distance is 4.66 Å. In the C2-α structures, the C-1 to C-2 bond is roughly *anti* to methyl-19, H-2β (or HO-2β) is disposed equatorially in the plane of the steroid and H-1β is roughly *anti* to H-2α. The H-2α to H-9 distance is much shorter: 2.54 Å. The calculated energy was about 4 kcal/mol lower for the C1-α conformer in all cases. Because solvent was not included in these calculations, and since it is well known[6,11] that 2β-hydroxylation of androst-4-ene-3-ones flips the A-ring from the C1-α to the C2-α form, the C2-α calculated structures were chosen to represent the 2β-hydroxylated compounds **1b**, **1d**, **2b** and **3b** and the C1-α structures were used to represent all others.

In the 2β-hydroxylated compounds **1b**, **1d**, **2b** and **3b** the C-2 to H-2α bond is almost perpendicular to the plane of the α,β-unsaturated ketone (average H-2α : C-2 : C-3 : O dihedral angle 96.8°), while the C-2 to OH bond is near the plane (22.5°). In the other compounds (**1a**, **1c**, **1e**, **2a** and **3a**) the situation is reversed: the average H-2α : C-2 : C-3 : O dihedral angle is 30.6° and the average H-2β : C-2 : C-3 : O dihedral angle is 84.9°. The C-6 to H-6β bond is roughly perpendicular to the plane; more so when there is no 2-hydroxy group (average H-6β : C-6 : C-5 : C-4 dihedral angle 100.1°) than for the 2β-hydroxylated compounds (125.9°). The C-6 to H-6α bond is close to the plane; more so for the 2β-hydroxylated compounds (average H-6α : C-6 : C-5 : C-4 dihedral angle 8.8°) than when there is no 2-hydroxy group (15.8°).

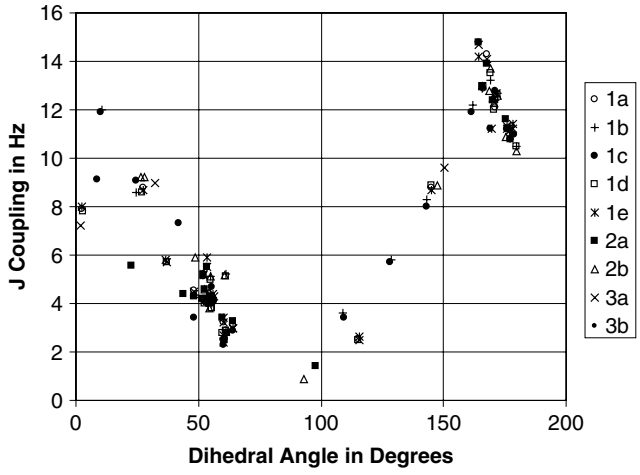

Figure 5. Plot of measured 3-bond (vicinal) ^{1}H–^{1}H *J* values vs dihedral angles from calculated structures.

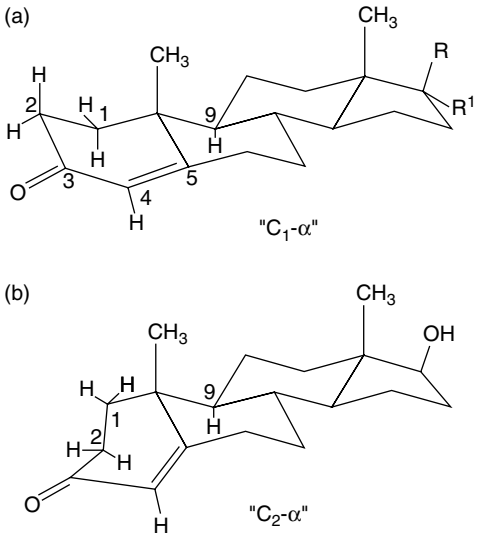

Figure 6. Structure diagrams for the C1-α (a) and C2-α (b) energy minima.

DISCUSSION

All steroid metabolites identified were hydroxylated at the 2, 12 or 15 positions of the steroid skeleton. In the nine products identified, hydroxylation occurred five times at position 15, four times at position 2 and twice at position 12. Furthermore, all 11 hydroxylations occurred on the β-face of the steroid, the same face as the angular methyl groups. This is also the same face as the substituent at position 17 in testosterone and progesterone. However, even with the planar 17-oxo substituent of androstenedione, we saw only β-face hydroxylation. This suggests that the cytochrome P450 (CYP6A1) enzyme binds steroid substrates with the β-face of the steroid facing the active oxygen species, but with either the A-ring or the D-ring end of the steroid inserted into the binding pocket.

It is well known that 2β-hydroxy-3-oxo-4-ene steroids adopt an A-ring conformation ('C2-α') which places the 2-OH group in a pseudo-equatorial position to avoid steric interaction with the 19-methyl group.[6,11] While our structure calculations showed two possible A-ring conformations, the C2-α conformation was higher in energy than the C1-α for all nine compounds studied, regardless of whether there was a 2β-OH substituent or not. Since the calculations were done in the absence of solvent, it is possible that solvation of the OH group adds to its steric bulk and favors the pseudo-equatorial position.

The conformational change of ring A from C1-α to C2-α interchanges the relationships of H-1α and H-1β to the plane of unsaturation, as well as interchanging their dihedral angles with H-2α. Thus NMR chemical shifts and vicinal couplings provide no evidence for the ring conformation, since the H-1α and H-1β assignments depend on the conformation. The observation of a strong NOE crosspeak between H-2α and H-9 in the 2β-hydroxylated steroid **1b** strongly supports the C2-α conformation (calculated distance

2.54 Å) over the C1-α conformation (calculated distance 4.66 Å). The absence of this crosspeak in **1a** provides evidence for the C1-α conformation in metabolites lacking a 2β-OH group. Further NMR evidence for the change in ring A conformation upon β-hydroxylation at C-2 is provided by long-range ^{1}H–^{1}H couplings and 2D-COSY correlations. A long-range COSY correlation is observed between H-1α and H-19Me for all but one of the compounds which lack a 2β-OH substituent, indicating that H-1α is *anti* to the angular methyl group (C1-α conformation). In the one exception (**2a**), the correlation cannot be observed due to resonance overlap. This correlation is missing in all of the 2β-hydroxy compounds because in the C2-α conformation both H-1α and H-1β are approximately *gauche* to Me-19. A COSY correlation between H-2α and H-4 is observed for **1a**, **1c**, **1e**, and **3a**, but is absent in the 2β-hydroxylated products **1b**, **1d**, **2b** and **3b** (this crosspeak is obscured in **2a** because of overlap). This is reflected in the H-4 resonance, which appears in resolution-enhanced spectra as a poorly resolved triplet or doublet of doublets for **1a, 1c, 1e, 2a** and **3a** but as a doublet for **1b, 1d, 2b** and **3b**. The H-2α to H-4 coupling is a W-coupling[29] and is absent in the 2β-OH series because the C-2 to H-2α bond is roughly perpendicular to the plane of C-2 : C-3 : C-4. The H-6β to H-4 (allylic) coupling is observed for all 9 metabolites in the 1D ^{1}H spectrum and the DQF-COSY, while the H-6α to H-4 COSY correlation is weak (**1d, 2b, 3a** and **3b**) or missing. Because the C_4–C_5 π bond is in the path of the coupling, the coupling is strongest when the H-6 to C-6 bond is perpendicular to the plane of the unsaturation.

Acknowledgements

We thank Dr Liliya Yatsunyk, who did the initial NMR work on compounds 2a and 2b. We thank Ronald C. Crouch of Varian NMR Systems Applications Laboratories, Palo Alto, CA, for providing the pulse sequence code for a 1,1-ADEQUATE experiment which uses ^{13}C broadband adiabatic refocusing and inversion shaped pulses. This work was supported by the National Institutes of Health grants GM39014 and ES06694 and by NSF U.S.-Hungary Collaborative Research grant INT-0 122 172.

REFERENCES

1. Guengerich FP, Shimada T. *Chem. Res. Toxicol.* 1991; **4**: 391.
2. Andersen JF, Utermohlen JG, Feyereisen R. *Biochemistry* 1994; **33**: 2171.
3. Andersen JF, Walding JK, Evans PH, Bowers WS, Feyereisen R. *Chem. Res. Toxicol.* 1997; **10**: 156.
4. Cerny I, Fajkos J, Pouzar V. *Steroids* 1996; **61**: 58; Mahato SB, Mukherjee A. *J. Steroid Biochem.* 1984; **21**: 341.
5. Kirk DN, Toms HC, Douglas C, White KA, Smith KE, Latif S, Hubbard RWP. *J. Chem. Soc., Perkin Trans. 2* 1990; 1567.
6. Kuriyama K, Kondo E, Tori K. *Tetrahedron Lett.* 1963; **22**: 1485.
7. Osawa Y, Gardner JO. *J. Org. Chem.* 1971; **36**: 3246.
8. Mineki S, Iida M, Kato K, Fukaya F, Kita K, Nakamura J, Yoshihama M. *J. Ferment. Bioeng.* 1995; **80**: 223.
9. Bednarski PJ, Nelson SD. *J. Med. Chem.* 1989; **32**: 203; Burnett RD, Kirk DN. *J. Chem. Soc., Perkin Trans. 1* 1973; **17**: 1830.
10. Tweit RC, Kagawa CM. *J. Med. Chem.* 1964; **53**: 524; Kawazoe Y, Sato Y, Okamoto T, Tsuda K. *Chem. Pharm. Bull.* 1963; **11**: 328.
11. Duax WL, Eger C, Pokrywiecki S, Osawa Y. *J. Med. Chem.* 1971; **14**: 295.
12. Bodenhausen G, Ruben DJ. *Chem. Phys. Lett.* 1980; **69**: 185.
13. Summers MF, Marzilli LG, Bax A. *J. Am. Chem. Soc.* 1986; **108**: 4285; Bax A, Marion D. *J. Magn. Reson.* 1988; **78**: 186.
14. Rance M, Sørensen OW, Bodenhausen G, Wagner G, Ernst RR, Wüthrich K. *Biochem. Biophys. Res. Commun.* 1983; **117**: 479.
15. Jeener J, Meier BH, Bachmann P, Ernst RR. *J. Chem. Phys.* 1979; **71**: 4546; Macura S, Ernst RR. *Mol. Phys.* 1980; **41**: 95.
16. Hurd RE, John BK. *J. Magn. Reson.* 1991; **91**: 648.
17. Willker W, Leibfritz D, Kerssebaum R, Bermel W. *Magn. Reson. Chem.* 1993; **31**: 287.
18. Sheng S, van Halbeek H. *J. Magn. Reson.* 1998; **130**: 296; Cicero DO, Barbato G, Bazzo R. *J. Magn. Reson.* 2001; **148**: 209; Edden RAE, Keeler J. *J. Magn. Reson.* 2004; **166**: 53.
19. Ding K. *Magn. Reson. Chem.* 2000; **38**: 321.
20. Abramovich D, Vega S. *J. Magn. Reson., Ser. A* 1993; **105**: 30.
21. Guzov VM, Houston HL, Murataliev MB, Walker FA, Feyereisen R. *J. Biol. Chem.* 1996; **271**: 26 637.
22. Murataliev MB, Arino A, Guzov VM, Feyereisen R. *Insect Biochem. Mol. Biol.* 1999; **29**: 233.
23. Marion D, Wüthrich K. *Biochem. Biophys. Res. Commun.* 1983; **113**: 967.
24. States DJ, Haberkorn RA, Ruben DJ. *J. Magn. Reson.* 1982; **48**: 286.
25. Ancian B, Bourgeois I, Dauphin J-F, Shaw AA. *J. Magn. Reson.* 1997; **125**: 348.
26. Cavanagh J, Palmer AG III, Wright PE, Rance M. *J. Magn. Reson.* 1991; **91**: 429.
27. Wimperis SC, Freeman R. *J. Magn. Reson.* 1984; **58**: 348.
28. Mackin G, Shaka AJ. *J. Magn. Reson., Ser. A* 1996; **118**: 247.
29. Barfield M. *Magn. Reson. Chem.* 2003; **41**: 344.

SUPPLEMENTARY MATERIAL

Supplementary material for this article is available at http://www.spectroscopyNOW.com/nmr/supplementary